

# Impact of relativistic chiral one-pion exchange on nuclear matter properties

Giuseppe Colucci,<sup>1</sup> Armen Sedrakian,<sup>1</sup> and Dirk H. Rischke<sup>1,2</sup>

<sup>1</sup>*Institute for Theoretical Physics, J. W. Goethe University,  
Max-von-Laue-Str. 1, D-60438 Frankfurt am Main, Germany*

<sup>2</sup>*Frankfurt Institute for Advanced Studies, Ruth Moufang Str. 1, D-60438 Frankfurt am Main, Germany*

We study nuclear matter properties in a model that features relativistic chiral one-pion exchange and contact interactions between nucleons. We apply thermal field theory methods to compute microscopically the nucleon self-energy arising from one-pion exchange and its contribution to the energy per nucleon in isospin-symmetric nuclear matter as well as neutron matter. The contact interactions are fitted to reproduce the energy density of isospin-symmetric nuclear matter at saturation as well as benchmark calculations for neutron matter. We find that relativistic one-pion exchange contributes about half of the binding energy of nuclear matter, the remainder being provided by the contact terms. We compare our model results to non-relativistic calculations based on low-momentum nucleon-nucleon potentials and discuss the symmetry energy and the compressibility of isospin-symmetric nuclear and neutron matter.

## I. INTRODUCTION

The equation of state of bulk nuclear matter has attracted considerable attention over time, as it has a substantial impact on the properties of neutron stars as well as finite nuclei. The equation of state is determined by two, generally related, ingredients: the force between nucleons and the many-body approximation used to compute the thermodynamic properties of nuclear matter. Nuclear interactions are accurately modeled in terms of potentials arising from meson exchange: on the one hand models have been used which are based on phase-shift equivalent one-boson exchange [1] and, on the other hand, more recently, (multi)-pion-exchange potentials based on chiral power counting [2]. The diversity of ab-initio many-body approaches includes variational Monte Carlo methods [3] and propagator methods with (medium-) renormalized soft interactions as, e.g., in non-relativistic and covariant Brueckner-type theories [4]. Hartree-Fock calculations of nuclear matter properties were revived with the advent of soft chiral potentials [5] which, however, require three- and four-body forces to account for contributions already included at the two-body level in the non-perturbative resummation schemes.

In this work we apply thermal field theory (TFT) methods to compute the equation of state of isospin-symmetric nuclear and neutron matter. The method has been applied in the past in the context of QED and QCD plasmas to compute the quasiparticle energies of electrons and quarks, respectively, in a thermal medium [6]. In the low-energy regime of interest to us, the relevant degrees of freedom are nucleons and pions. Chiral symmetry is an (approximate) symmetry of the strong interaction. Because the chiral symmetry is spontaneously broken in Nature, pions emerge as the (pseudo-) Goldstone bosons of the theory. The description of the strong interaction in terms of chiral Lagrangians admits certain approximation schemes in terms of power counting of small quantities [7, 8], which in principle allow for a

systematic order-by-order improvement of a given calculation. Below, we will combine relativistic TFT methods and the chiral Lagrangian description of nuclear interactions to address the computation of thermodynamic properties of nuclear and neutron matter.

Approaches similar to ours were previously developed in Refs. [9–11]. Fraga et al. [9] derived analytical expressions for the zero-temperature self-energy of a nucleon due to pion exchange in dilute nuclear matter to leading order in the chiral expansion (but they did not address nuclear saturation). Lutz et al. [10] and Kaiser et al. [11] used chiral Lagrangians and expansions in small Fermi momentum to construct equations of state in the heavy-baryon limit. The saturation in Ref. [10] arises due to correlations induced by the one-pion-exchange interaction. In Ref. [11] two-pion exchange produces nuclear binding at three-loop level with a suitably adjusted momentum cut-off.

In applying TFT to nuclear matter in a relativistic setting, we have to maintain the covariance of the theory by using fully relativistic thermal propagators for nucleons and pions. Keeping the Lorentz symmetries intact is of advantage, in particular, for computing the scattering and radiation amplitudes with full propagators and renormalized vertices. The second goal of our work is to maintain self-consistency among the propagators and the self-energies of the theory, which means that the iterations are performed until the Schwinger-Dyson equation for the nucleons is fulfilled. If a firm perturbative expansion (with power-counting rules) exists, a self-consistent approach generates higher-order terms in every iteration, and therefore is not really necessary. Nevertheless, using the leading-order term in the chiral expansion of the Lagrangian, we will check the impact of these higher-order terms in a self-consistent solution. Third, we shall address the role of the two- and three-body contact terms which are necessary to achieve nuclear saturation in isospin-symmetric nuclear matter and we shall discuss some of the key nuclear observables such as the symmetry energy and the compressibility.

This paper is structured as follows. In Sec. II we dis-

cuss the chiral Lagrangian. Section III uses TFT to compute the pion contribution to the nucleon self-energy. Our numerical method and results for the self-energy as well as nuclear matter properties are presented in Sec. IV. Our conclusions are collected in Sec. V. We use natural units  $\hbar = c = k_B = 1$ . Four-vectors are denoted with capital letters, for instance  $P^\mu = (p^0, \mathbf{p})$ .

## II. LAGRANGIANS

Low-energy nuclear dynamics can be constructed on the basis of the pion and nucleon degrees of freedom starting from a chiral Lagrangian. The interaction Lagrangian  $\mathcal{L}_{\pi N}$  between nucleons and pions is constructed such as to reflect the spontaneous chiral symmetry breaking of strong interactions at low energies. Since the interactions of Goldstone bosons must vanish at zero-momentum transfer and in the chiral limit (i.e., the pion mass  $m_\pi \rightarrow 0$ ), a low-energy expansion in powers (the so-called chiral dimension) of the ratio of the momentum or the pion mass over (4 $\pi$  times) the pion-decay constant can be performed. Consequently, the Lagrangian can be written as

$$\mathcal{L}_{\pi N} = \mathcal{L}_{\pi N}^{(1)} + \mathcal{L}_{\pi N}^{(2)} + \dots, \quad (1)$$

where the superscript labels the order of the chiral dimension. The terms in the expansion (1) are constructed by introducing the following  $SU(2)$  matrix  $U$  in flavor space

$$U = \exp \left( i \frac{\boldsymbol{\tau} \cdot \boldsymbol{\pi}}{f_\pi} \right) = 1 + \frac{i}{f_\pi} \boldsymbol{\tau} \cdot \boldsymbol{\pi} - \frac{1}{2f_\pi^2} \boldsymbol{\pi}^2 + \dots, \quad (2)$$

where  $\boldsymbol{\tau}$  is vector of Pauli matrices in isospin space,  $\boldsymbol{\pi}$  is the isotriplet of pions, and  $f_\pi$  the pion decay constant. The leading-order term is given by [12]

$$\mathcal{L}_{\pi N}^{(1)} = \bar{\psi} \left( i \gamma^\mu D_\mu - m + \frac{g_A}{2} \gamma^\mu \gamma_5 u_\mu \right) \psi, \quad (3)$$

where  $\psi$  is the nucleon field,  $\bar{\psi} = \psi^\dagger \gamma_0$ ,  $m$  is the nucleon mass, and  $g_A$  is the axial-vector coupling. The physical value of  $g_A$  is determined from neutron beta decay and is given by  $g_A = 1.2695 \pm 0.0029$ .  $D_\mu$  is the covariant derivative,

$$D_\mu = \partial_\mu + \Gamma_\mu \quad (4)$$

where  $\Gamma_\mu$  is the so-called chiral connection which couples an even number of pions to the nucleon and is defined as

$$\begin{aligned} \Gamma_\mu &= i[\xi^\dagger, \partial_\mu \xi] = i(\xi^\dagger \partial_\mu \xi + \xi \partial_\mu \xi^\dagger) \\ &= -\frac{1}{4f_\pi^2} \boldsymbol{\tau} \cdot (\boldsymbol{\pi} \times \partial_\mu \boldsymbol{\pi}) + \dots \end{aligned} \quad (5)$$

with  $\xi = \sqrt{U}$ . The Lagrangian (3) also includes the axial-vector current  $u_\mu$  which couples an odd number of pions to the nucleon

$$u_\mu = i[\xi^\dagger, \partial_\mu \xi] = i(\xi^\dagger \partial_\mu \xi - \xi \partial_\mu \xi^\dagger) = -\frac{1}{f_\pi} \boldsymbol{\tau} \cdot \partial_\mu \boldsymbol{\pi} + \dots \quad (6)$$

Keeping only the lowest-order term in the chiral Lagrangian (3) the pion-nucleon Lagrangian reads [2]

$$\mathcal{L}_{\pi N}^{(1)} = \bar{\psi} \left( i \gamma^\mu \partial_\mu - m - \frac{g_A}{2f_\pi} \gamma^\mu \gamma_5 \boldsymbol{\tau} \cdot \partial_\mu \boldsymbol{\pi} \right) \psi, \quad (7)$$

where we have neglected the Weinberg-Tomozawa contribution arising from the chiral connection (5). The chiral one-pion interaction term in Eq. (7) takes the light dynamical degrees of freedom, *i.e.*, pions, explicitly into account. The complete interaction Lagrangian includes, in addition, the four-fermion and, in addition, the six-fermion contact interaction, respectively, which become important at high density. Thus, the Lagrangian of the system can be written as

$$\mathcal{L} = \mathcal{L}_{\text{free}} + \mathcal{L}_{\pi N}^{(1)} + \mathcal{L}_{NN} + \mathcal{L}_{NNN}, \quad (8)$$

where the first term is the Lagrangian of the non-interacting system and the last two terms correspond to the two-body and three-body interactions. Figure 1 shows the three distinct contributions to the self-energy of a nucleon originating from the tree-level vertices in the Lagrangian (8).

## III. PION CONTRIBUTION TO THE SELF-ENERGY

### A. Leading-order contribution

In this section we evaluate the one-pion contribution to the nucleon self-energy, corresponding to the left diagram in Fig. 1, within the imaginary-time formalism. The free covariant propagator of the nucleons in energy-momentum space is given by

$$S_0(K) = \frac{\Lambda_k^+ \gamma_0}{ik_n + \mu - E_k} + \frac{\Lambda_k^- \gamma_0}{ik_n + \mu + E_k}, \quad (9)$$

where the zeroth component of the four-momentum  $K^\mu \equiv (k^0, \mathbf{k})$  takes discrete values,  $k^0 = ik_n = (2n + 1)\pi iT$ ,  $n \in \mathbb{Z}$  and  $T$  is the temperature.  $\Lambda_k^\pm$  are projectors onto positive (+) and negative (-) energy states,

$$\Lambda_k^\pm = \frac{1}{2E_k} [E_k \pm (\boldsymbol{\alpha} \cdot \mathbf{k} + m\gamma_0)], \quad (10)$$

where  $E_k^2 = \mathbf{k}^2 + m^2$  is the dispersion relation for non-interacting nucleons,  $m$  is their mass, and  $\boldsymbol{\alpha} \equiv \gamma_0 \boldsymbol{\gamma}$ . The free pion propagator is given by

$$D_0(Q) = \frac{1}{2\omega_q} \left( \frac{1}{i\omega_n - \omega_q} - \frac{1}{i\omega_n + \omega_q} \right), \quad (11)$$

where the zeroth component of the four-momentum  $Q^\mu \equiv (q^0, \mathbf{q})$  takes discrete values  $q^0 = i\omega_n = 2n\pi iT$ ,  $n \in \mathbb{Z}$ , and  $\omega_q^2 = q^2 + m_\pi^2$  is the dispersion relation for non-interacting pions, with  $m_\pi$  being the free pion mass. In

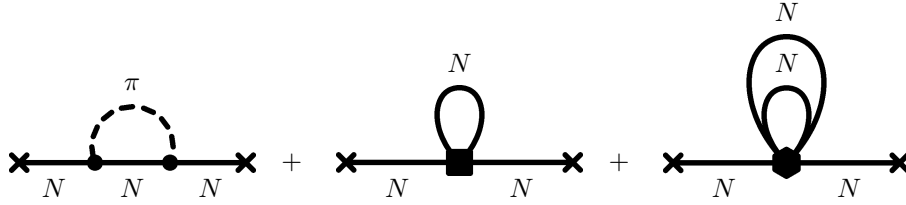


FIG. 1. The three diagrams contributing to the self-energy of the nucleon. The first one represents the chiral one-pion exchange contribution to the nucleon self-energy. Solid lines refer to nucleons, dashed lines to pions and dots to pion-nucleon vertices. The second diagram is the contribution from the two-body contact interaction, with the square vertex representing the two-body scattering matrix. The third diagram is the contribution from the three-body interactions with the hexagonal vertex representing the three-body scattering matrix. In each diagram the external legs do not contribute to the self-energy.

terms of the free propagators (9) and (11) the one-pion exchange contribution to the nucleon self-energy reads

$$\Sigma(P) = -\frac{3g_A^2}{4f_\pi^2} T \int \frac{d^3 \mathbf{k}}{(2\pi)^3} \sum_{ik_n} D_0(P - K) \gamma_5(\not{P} - \not{K}) \times S_0(K) \gamma_5(\not{P} - \not{K}), \quad (12)$$

where  $P^\mu = (p^0, \mathbf{p}) \equiv (ip_n, \mathbf{p})$ . We substitute the propagators (9) and (11) into Eq. (12) and carry out the summation over the fermionic Matsubara frequency  $ik_n$ . In general, this sum generates physically distinct processes involving all possible combinations of bosons and fermions and their antiparticles. The result of the summation can be arranged according to these underlying processes, but it is more convenient to separate

the self-energy into the “vacuum” and “thermal” parts  $\Sigma(P) = \Sigma_0(P) + \Sigma_T(P)$ , where the vacuum part is given by

$$\Sigma_0(P) = \frac{3g_A^2}{4f_\pi^2} \int \frac{d^3 \mathbf{k}}{(2\pi)^3} \frac{1}{2\omega_{pk}} \times \left[ \frac{\gamma_5(\not{P} - \not{K}) \Lambda_k^+ \gamma_0 \gamma_5(\not{P} - \not{K})}{ip_n + \mu - E_k - \omega_{pk}} \Big|_{k_0=ip_n - \omega_{pk}} \right. \\ \left. + \frac{\gamma_5(\not{P} - \not{K}) \Lambda_k^- \gamma_0 \gamma_5(\not{P} - \not{K})}{ip_n + \mu + E_k + \omega_{pk}} \Big|_{k_0=E_k + \mu} \right], \quad (13)$$

and the thermal part is given by

$$\Sigma_T(P) = \frac{3g_A^2}{4f_\pi^2} \int \frac{d^3 \mathbf{k}}{(2\pi)^3} \frac{1}{2\omega_{pk}} \left\{ \left[ \frac{1}{ip_n + \mu - E_k - \omega_{pk}} - \frac{1}{ip_n + \mu - E_k + \omega_{pk}} \right] \gamma_5(\not{P} - \not{K}) \Lambda_k^+ \gamma_0 \gamma_5(\not{P} - \not{K}) \Big|_{k_0=E_k - \mu} n_F(E_k - \mu) \right. \\ - \left[ \frac{1}{ip_n + \mu + E_k - \omega_{pk}} - \frac{1}{ip_n + \mu + E_k + \omega_{pk}} \right] \gamma_5(\not{P} - \not{K}) \Lambda_k^- \gamma_0 \gamma_5(\not{P} - \not{K}) \Big|_{k_0=-E_k - \mu} n_F(E_k - \mu) \\ - \gamma_5(\not{P} - \not{K}) \left[ \frac{\Lambda_k^+ \gamma_0}{ip_n + \mu - E_k - \omega_{pk}} + \frac{\Lambda_k^- \gamma_0}{ip_n + \mu + E_k - \omega_{pk}} \right] \gamma_5(\not{P} - \not{K}) \Big|_{k_0=ip_n - \omega_{pk}} n_B(\omega_{pk}) \\ \left. - \gamma_5(\not{P} - \not{K}) \left[ \frac{\Lambda_k^+ \gamma_0}{ip_n + \mu - E_k + \omega_{pk}} + \frac{\Lambda_k^- \gamma_0}{ip_n + \mu + E_k + \omega_{pk}} \right] \gamma_5(\not{P} - \not{K}) \Big|_{k_0=ip_n + \omega_{pk}} n_B(\omega_{pk}) \right\}, \quad (14)$$

where  $\omega_{pk}^2 = (\mathbf{p} - \mathbf{k})^2 + m_\pi^2$  and  $n_{F/B}(x) = [\exp(x/T) \pm 1]^{-1}$  are the Fermi/Bose distribution functions. The retarded self-energy is obtained by analytical continuation, *i.e.*,  $ip_n \rightarrow p_0 + i0^+$ . We have verified that in the case of a Yukawa interaction Eq. (14) transforms to the well-known expression for the self-energy of a fermion in finite-temperature quantum field theory [6, 13].

At sufficiently low temperature the occupation number of anti-particles is so small that we can neglect their contribution in Eq. (14). Furthermore, we assume that there is no macroscopic occupation of pionic modes in nuclear matter at any temperature and density of interest; therefore, we also drop the contributions proportional to the bosonic occupation numbers. The remaining contribution arises from the pole at  $k_0 \equiv E_k - \mu$  and we arrive at

$$\Sigma_T(P) = -\frac{3g_A^2}{4f_\pi^2} \int \frac{d^3 \mathbf{k}}{(2\pi)^3} \frac{1}{2\omega_{pk}} \left[ \frac{1}{p_0 - k_0 - \omega_{pk} + i0^+} - \frac{1}{p_0 - k_0 + \omega_{pk} + i0^+} \right] (s + \not{Q}) n_F(k_0), \quad (15)$$

where we have defined the quantities  $s = -(m/2E_k)(P - K)^2$  and  $Q^\mu = (q_0, \mathbf{q})$ , with components

$$q_0 = \frac{1}{2}[(p_0 - k_0)^2 + (\mathbf{p} - \mathbf{k})^2] - \frac{1}{E_k}(\mathbf{p} - \mathbf{k}) \cdot \mathbf{k}(p_0 - k_0) , \quad (16)$$

$$\mathbf{q} = -\frac{1}{2E_k} [(P - K)^2 \mathbf{k} + 2(\mathbf{p} - \mathbf{k}) \cdot \mathbf{k}(\mathbf{p} - \mathbf{k})] + (p_0 - k_0)(\mathbf{p} - \mathbf{k}) . \quad (17)$$

Later on we will enforce self-consistency in evaluating the self-energy. This requires a Lorentz decomposition of the self-energy, which in the most general case is given by

$$\Sigma(P) = \Sigma_s(P) + \gamma_5 \Sigma_{ps}(P) + \gamma^\mu \Sigma_\mu(P) + \gamma_5 \gamma^\mu \Sigma_\mu^A(P) + \sigma^{\mu\nu} \Sigma_{\mu\nu}(P) . \quad (18)$$

The requirements of parity conservation, translational and rotational invariance, as well as time-reversal invariance, reduce this most general decomposition to the following form

$$\Sigma(P) = \Sigma_s(P) + \gamma_0 \Sigma_0(P) + \boldsymbol{\gamma} \cdot \mathbf{p} \Sigma_v(P) . \quad (19)$$

Equation (15) can now be projected onto its Lorentz components by multiplying it with  $1, \gamma_0$ , and  $\boldsymbol{\gamma}$ , and taking the trace over the  $\gamma$ -matrices. Keeping only the thermal part of the self-energy (and dropping the index  $T$  on the self-energies), this leads us to the following decomposition coefficients

$$\Sigma_s(P) = \frac{3g_A^2}{4f_\pi^2} \int \frac{d^3\mathbf{k}}{(2\pi)^3} \frac{1}{2\omega_{pk}} \left[ \frac{1}{p_0 - k_0 - \omega_{pk} + i0^+} - \frac{1}{p_0 - k_0 + \omega_{pk} + i0^+} \right] n_F(k_0) \frac{m}{2E_k} (P - K)^2 , \quad (20)$$

$$\begin{aligned} \Sigma_0(P) = & -\frac{3g_A^2}{4f_\pi^2} \int \frac{d^3\mathbf{k}}{(2\pi)^3} \frac{1}{2\omega_{pk}} \left[ \frac{1}{p_0 - k_0 - \omega_{pk} + i0^+} - \frac{1}{p_0 - k_0 + \omega_{pk} + i0^+} \right] n_F(k_0) \\ & \times \left[ \frac{1}{2}((p_0 - k_0)^2 + (\mathbf{p} - \mathbf{k})^2) + \frac{1}{E_k}(\mathbf{p} - \mathbf{k}) \cdot \mathbf{k}(p_0 - k_0) \right] , \end{aligned} \quad (21)$$

$$\begin{aligned} \mathbf{p} \Sigma_v(P) = & -\frac{3g_A^2}{4f_\pi^2} \int \frac{d^3\mathbf{k}}{(2\pi)^3} \frac{1}{2\omega_{pk}} \left[ \frac{1}{p_0 - k_0 - \omega_{pk} + i0^+} - \frac{1}{p_0 - k_0 + \omega_{pk} + i0^+} \right] n_F(k_0) \\ & \times \left\{ \frac{1}{2E_k} [(P - K)^2 \mathbf{k} + 2(\mathbf{p} - \mathbf{k}) \cdot \mathbf{k}(\mathbf{p} - \mathbf{k})] - (p_0 - k_0)(\mathbf{p} - \mathbf{k}) \right\} \cdot \hat{\mathbf{p}} , \end{aligned} \quad (22)$$

where  $\hat{\mathbf{p}} = \mathbf{p}/|\mathbf{p}|$  is a unit vector. Equations (20)–(22) are our final result for the chiral one-pion-exchange to the nucleon self-energy. It is evident that the other terms in Eq. (14), which could become important at higher temperatures and densities, can be evaluated in a completely analogous way.

## B. Further approximations

For numerical computations the factor  $(s + Q)$  in Eq. (15) can be simplified. We start by rewriting the expression

$$\begin{aligned} 2E_k Q = & 2E_k(q_0 \gamma_0 - \mathbf{q} \cdot \boldsymbol{\gamma}) = \mu [(p_0 - k_0)^2 + (\mathbf{p} - \mathbf{k})^2] \gamma_0 \\ & + 2(P - K) \cdot K \hat{\mathbf{p}} - (P^2 - K^2) K \\ & - 2\mu(p_0 - k_0)(\mathbf{p} - \mathbf{k}) \cdot \boldsymbol{\gamma} . \end{aligned} \quad (23)$$

For the densities and temperatures of interest, nucleons are constrained to the vicinity of their Fermi surface, therefore the momentum of the nucleon can be expressed as  $\mathbf{p} = p_F \hat{\mathbf{n}} + \delta \mathbf{p}$ . Here,  $p_F$  is the nucleon Fermi momentum,  $\hat{\mathbf{n}}$  is a unit vector, and  $\delta \mathbf{p}$  is the residual momentum, with  $|\delta \mathbf{p}| \ll p_F$ . Furthermore, the relativity parameter  $x = p_F/m$  is small as well; numerically, we have

$$x \approx 0.28 \left( \frac{n}{n_0} \right)^{1/3} , \quad (24)$$

where  $n$  is the density of the systems,  $n_0 = 0.16 \text{ fm}^{-3}$  is the nuclear saturation density. Then, the nucleon energy is  $E_p \approx m(1 + \mathbf{p}^2/2m^2)$  and the chemical potential  $\mu \approx m(1 + p_F^2/2m^2)$ . This implies that  $p_0 = E_p - \mu \approx (\mathbf{p}^2 - p_F^2)/2m \approx x \hat{\mathbf{n}} \cdot \delta \mathbf{p}$  is small compared to  $|\mathbf{p}| \approx p_F$ . Therefore, we can replace  $(P - K)^2 \approx -(\mathbf{p} - \mathbf{k})^2$ .

With these approximations we obtain

$$\begin{aligned} 2E_k Q \approx & 2m Q \approx \mu(\mathbf{p} - \mathbf{k})^2 \gamma_0 - 2(\mathbf{p} - \mathbf{k}) \cdot \mathbf{k} \hat{\mathbf{p}} \\ & + (\mathbf{p}^2 - \mathbf{k}^2) K - (\mathbf{p}^2 - \mathbf{k}^2)(\mathbf{p} - \mathbf{k}) \cdot \boldsymbol{\gamma} \\ & \approx (\mathbf{p} - \mathbf{k})^2 [(p_0 + \mu)\gamma_0 - \mathbf{p} \cdot \boldsymbol{\gamma}] \end{aligned} \quad (25)$$

where we used the fact that  $p_0 - k_0 \approx (\mathbf{p}^2 - p_F^2)/2m - (\mathbf{k}^2 - p_F^2)/2m = (\mathbf{p}^2 - \mathbf{k}^2)/2m$ .

Therefore, the factor  $s + Q$  in the integrand of the self-energy (15) reads now

$$s + Q \approx \frac{(\mathbf{p} - \mathbf{k})^2}{2m} [m + (p_0 + \mu)\gamma_0 - \boldsymbol{\gamma} \cdot \mathbf{p}] . \quad (26)$$

Separating the contributions from particles and anti-particles in the boson propagator, with these approxima-

tions the self-energy reads

$$\begin{aligned}\Sigma(P) &\approx [m + (p_0 + \mu)\gamma_0 - \boldsymbol{\gamma} \cdot \mathbf{p}] [\sigma_+(P) + \sigma_-(P)] \\ &\equiv [m + (p_0 + \mu)\gamma_0 - \boldsymbol{\gamma} \cdot \mathbf{p}] \sigma(P),\end{aligned}\quad (27)$$

where

$$\sigma_{\pm}(P) = \mp \frac{3g_A^2}{8mf_{\pi}^2} \int \frac{d^3\mathbf{k}}{(2\pi)^3} \frac{1}{2\omega_{pk}} \frac{(\mathbf{p} - \mathbf{k})^2}{p_0 - k_0 \mp \omega_{pk} + i\eta} n_F(k_0). \quad (28)$$

Therefore, the coefficients of the Lorentz decomposition of the self-energy can be expressed in terms of  $\sigma(p)$ ,

$$\begin{aligned}\Sigma_s(P) &\approx m\sigma(P), \quad \Sigma_0(P) \approx (p_0 + \mu)\sigma(P), \\ \Sigma_v(P) &\approx -\sigma(P).\end{aligned}\quad (29)$$

The real part of the self-energy can now be computed with the help of the Dirac identity. We obtain by explicitly evaluating the Cauchy principal value of Eq. (28)

$$\begin{aligned}\text{Re}[\sigma(P)] &\equiv \text{Re}[\sigma_+(P) + \sigma_-(P)] \\ &= -\frac{3g_A^2}{32m\pi^2 f_{\pi}^2} \int_0^{\infty} d|\mathbf{k}| \mathbf{k}^2 \frac{n_F(k_0)}{2|\mathbf{p}||\mathbf{k}|} \int_{-1}^1 dx \frac{(\mathbf{p} - \mathbf{k})^2}{x - x_0}\end{aligned}\quad (30)$$

where  $x_0 = [\mathbf{p}^2 + \mathbf{k}^2 + m_{\pi}^2 - (p_0 - k_0)^2]/(2|\mathbf{p}||\mathbf{k}|)$ .

### C. Enforcing self-consistency

The self-consistency of the numerical computation of the self-energy is achieved by replacing the free nucleon propagator in Eq. (12) by the full nucleon propagator, determined by the Schwinger-Dyson equation

$$S^{-1}(P) = S_0^{-1}(P) - \Sigma(P) = [(p_0 + \mu)\gamma_0 - \boldsymbol{\gamma} \cdot \mathbf{p}][1 - \text{Re}\sigma(P)]$$

where the free nucleon propagator is given by  $S_0^{-1}(P) = (p_0 + \mu)\gamma_0 - \boldsymbol{\gamma} \cdot \mathbf{p} - m$  and we have used Eq. (27) for the nucleon self-energy. The roots of  $\det S^{-1}(P)$  determine the excitation spectrum of the system,

$$p_0^* = E_p^* - \mu^*, \quad (32)$$

where

$$E_p^* = \sqrt{\mathbf{p}^{*2} + m^{*2}}, \quad (33)$$

$$m^* = m[1 + \text{Re}\sigma(P^*)], \quad (34)$$

$$\mathbf{p}^* = \mathbf{p}[1 - \text{Re}\sigma(P^*)], \quad (35)$$

$$\mu^* = \mu[1 - \text{Re}\sigma(P^*)]. \quad (36)$$

We achieve self-consistency for the self-energy by replacing the free quantities  $m$ ,  $\mathbf{p}$ ,  $\mathbf{k}$ , and  $\mu$  in the integrand (but not in the integration measure) of Eq. (30) by the corresponding renormalized  $m^*$ ,  $\mathbf{p}^*$ ,  $\mathbf{k}^*$ , and  $\mu^*$ . In practice, we start by computing (30) with the free quantities, which define the renormalized quantities (33)–(36) to first order in the iteration process. We repeat the previous step until convergence is reached.

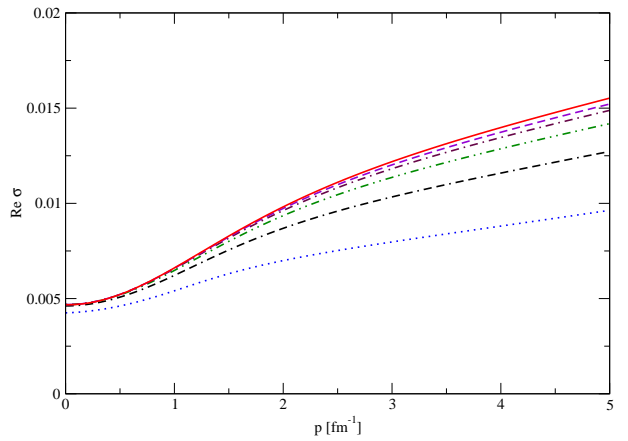


FIG. 2. (Color online) Real part of the nucleon self-energy as a function of momentum  $p$  at  $n = 0.1 \text{ fm}^{-3}$  and  $T = 0$ . The dotted (blue) line is the lowest-order result and simultaneously the starting point of the iteration. The full (red) line represents the final self-consistent result. The other lines correspond to 2,3,4,5 (from bottom to top) iteration steps.

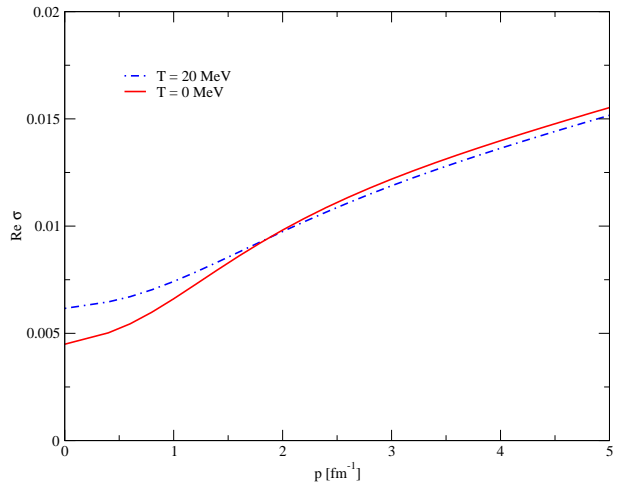


FIG. 3. (Color online) Dependence of the one-pion exchange contribution to the nucleon self-energy in isospin-symmetric nuclear matter on the momentum at density  $n = 0.1 \text{ fm}^{-3}$ . The solid line shows the real part of the self-energy for temperature  $T = 0$  and the dashed-dotted line for  $T = 20 \text{ MeV}$ .

## IV. RESULTS

The energy per nucleon, excluding its rest mass  $m$ , is defined as

$$\frac{E}{N} = \mathcal{T} + \mathcal{U} - m, \quad (37)$$

where  $\mathcal{T}$  is the kinetic energy,  $\mathcal{U}$  the single-particle potential and  $N$  is the particle number. In terms of the renor-

	BHF	SCGF	$V_{\text{low-}k}$	ChPT
$t_0$ [MeV fm $^3$ ]	-153	-311	-438.1	-836.052
$t_3$ [MeV fm $^{3+3\alpha}$ ]	2720	3670	6248	8048.29

TABLE I. Parameters  $t_0$  and  $t_3$  defining the contact interaction of Eq. (40) as obtained from a fit to the saturation point  $n_0 = 0.16 \text{ fm}^{-3}$  and  $E/N = -16.0 \text{ MeV}$  at  $\alpha = 0.5$  for different models of nuclear matter [14].

malized quantities (34)–(36) the kinetic energy reads

$$\mathcal{T} = \frac{g_\tau}{\pi^2 n} \int d|\mathbf{p}| \mathbf{p}^2 \left( \frac{m^*}{E_p^*} m + \frac{|\mathbf{p}^*|}{E_p^*} |\mathbf{p}| \right) n_F(E_p^* - \mu^*), \quad (38)$$

where  $g_\tau$  is the isospin degeneracy factor ( $g_\tau = 2$  in isospin-symmetric nuclear matter and  $g_\tau = 1$  in neutron matter). The single-particle potential,  $\mathcal{U}$ , is given by

$$\mathcal{U} = \frac{g_\tau}{2\pi^2 n} \int d|\mathbf{p}| \mathbf{p}^2 \left[ \frac{m^*}{E_p^*} m + E_p - \frac{|\mathbf{p}^*|}{E_p^*} |\mathbf{p}| \right] \times \sigma(P) n_F(E_p^* - \mu^*). \quad (39)$$

As we consider only spin-unpolarized matter, the spin summation has been carried out in Eqs. (38) and (39).

### A. Symmetric nuclear matter

The Fock diagram evaluated in the previous section represents chiral one-pion exchange between two nucleons, therefore its contribution to the potential energy is attractive. In order to achieve saturation in symmetric nuclear matter, we need to add a potential which includes the self-energy contribution arising from the two- and three-nucleon contact interactions, shown in Fig. 1. This contribution can be expressed in the form of a Skyrme-like interaction, given by

$$V_c(\rho) = \frac{1}{2} t_0 n + \frac{1}{12} t_3 n^{1+\alpha}, \quad (40)$$

where  $n$  is the density and  $t_0$ ,  $t_3$ , and  $\alpha$  are parameters. For a fixed value of  $\alpha$  (typically  $\alpha = 0.5$ ), we fit  $t_0$  and  $t_3$  in such a way that Eq. (37) yields the empirical saturation point for symmetric nuclear matter. For  $\alpha = 0.5$ , the fit results in an attractive two-body contact interaction ( $t_0 < 0$ ) and a repulsive three-body one ( $t_3 > 0$ ). The numerical values for  $t_0$  and  $t_3$  are given in Table I. We note that the value of  $\alpha$  controls the stiffness of the equation of state at high densities, with larger values corresponding to a stiffer equation of state. The particular value  $\alpha = 0.5$  is consistent with the density-dependent part of the Skyrme interaction.

Once the parameters are fixed, we compute the nuclear compressibility modulus, defined as

$$K = 9n^2 \frac{\partial^2(E/N)}{\partial n^2} \Big|_{n=n_0}. \quad (41)$$

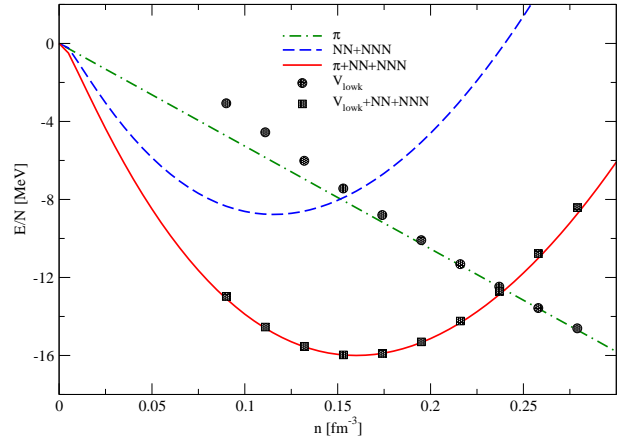


FIG. 4. (Color online) Dependence of the energy per nucleon in symmetric nuclear matter on density at  $T = 0$  (solid red line). The chiral one-pion exchange contribution to the potential energy is shown by the dashed-dotted (green) line and the contribution from contact terms by the dashed (blue) line. For comparison, we show the one-pion exchange contribution (dots) as well as the full result (squares) from calculations using a low-momentum potential  $V_{\text{low-}k}$ .

We find  $K \approx 267 \text{ MeV}$ , which is in agreement with the empirically known value ( $K \approx 250 \pm 25 \text{ MeV}$ ).

The self-energy due to chiral one-pion exchange in isospin-symmetric nuclear matter is shown in Fig. 2 at  $T = 0$  and  $n = 0.1 \text{ fm}^{-3}$ . As one observes, the self-consistency procedure converges rapidly. In order to achieve a relative accuracy  $\leq 10^{-6}$  one needs about 10 iterations, the exact number of iteration depending on the density. For small densities the number of required iterations is small, while for large densities the number of iterations needed to achieve convergence is larger. While the self-energy does not tend to zero for large external momenta, the result for the energy of the system is convergent due to an additional integration over a Fermi distribution function.

In Fig. 3 we show the self-energy at zero temperature in comparison to its form at  $T = 20 \text{ MeV}$ . The change with temperature can be seen to be rather moderate. In the non-zero temperature case the self-energy is larger for low momenta than at zero temperature, while for higher momenta the variation of temperature does not affect the result very much. This is due to the fact that we deal with comparatively low temperatures, therefore the temperature is a relevant scale only at low momenta.

It can be seen from the expression of the self-energy in Eq. (27) and from the definition of the self-energy coefficients (29), that the vector self-energy is substantially smaller than the other contributions to the self-energy, as expected. Our numerical result for the real part of the reduced self-energy is in good agreement with the one quoted by Ref. [9] in their zero-temperature calculations.

The energy per nucleon in isospin-symmetric nuclear matter at  $T = 0$  is shown in Fig. 4 along with its potential-energy components which are split into the con-

tribution of one-pion exchange and the contribution from two- and three-body contact interactions. The one-pion exchange contribution is linear in the density, as one would expect from a mean-field type contribution and is always negative, as it reflects the attractive interaction between nucleons. The two-body contact interaction is attractive, while the three-body interaction is repulsive. As stated above, the parameters of these interaction were chosen to fit the saturation point of nuclear matter. It is remarkable that quantitatively the contact interactions make a substantial contribution at all densities of interest, therefore one may conclude that the relativistic one-pion exchange alone cannot account for the attraction in isospin-symmetric nuclear matter and cannot lead to the correct saturation properties in combination with only repulsive three-body forces acting at high densities. In the limit of vanishing density the kinetic energy becomes dominant and we recover the free Fermi gas behavior of the energy.

Figure 4 also shows a comparison of the energies per nucleon in isospin-symmetric nuclear matter in our case and in the model which uses the  $V_{\text{low-}k}$  interaction. The latter one is a soft, phase-shift equivalent interaction which applies below some momentum cut-off. As can be seen, this model also requires a potential-energy contribution from two- and three-body contact interactions in order to achieve saturation of nuclear matter. The models agree well (per fit of the contact interactions) for the energy per nucleon, but in both cases a substantial portion of the attractive energy has to be included in the phenomenological two-body contact term, in order to reproduce the phenomenological features of isospin-symmetric nuclear matter.

The compressibility in our model is  $K = 267$  MeV, which is in good agreement with the one predicted by the  $V_{\text{low-}k}$  interaction ( $K = 258$  MeV). Table I compares the parameters of the two- and three-body contact interactions required to fit the nuclear saturation point in isospin-symmetric nuclear matter for several models. Indeed, all non-relativistic models overbind nuclear matter at the saturation density, therefore repulsive three-body forces are mandatory to cure this problem. It is seen that the values used in the literature and those in our fits are more or less of the same order of magnitude and, for instance, the ratios between the parameters in our model to those of the  $V_{\text{low-}k}$  interaction are  $\sim 2$  for  $t_0$  and  $4/3$  for  $t_3$ .

### B. Pure neutron matter

The self-energy of neutrons in pure neutron matter is shown in Fig. 5. Compared to isospin-symmetric nuclear matter, the self-energy in neutron matter is smaller. This is due to the fact that in pure neutron matter the one-pion exchange involves only the  $\pi^0$ -meson. At non-zero temperature, as in the case of isospin-symmetric nuclear matter, we observe that, for low momenta, the contri-

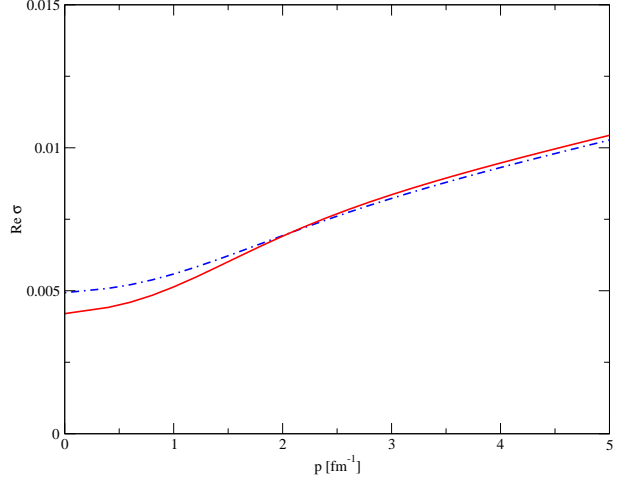


FIG. 5. (Color online) Dependence of the one-pion exchange contribution to the nucleon self-energy in pure matter on the momentum, at density  $n = 0.1 \text{ fm}^{-3}$ . The solid line shows the real part of the self-energy for temperature  $T = 0$  while the dot-dashed line - for  $T = 20 \text{ MeV}$ .

bution of the self-energy at higher temperature is larger, but the difference among the two cases tends to disappear with increasing momentum.

The energy per particle in pure neutron matter is shown in Fig. 6. Now we fit the parameters at two values of the density, namely at saturation and at twice the saturation density, to the quantum Monte-Carlo calculations of Ref. [15], which are based on the Argonne AV8' two-body and Urbana IX three-body forces. The attractive contribution from chiral one-pion exchange is smaller in this case, due to the smallness of the neutron self-energy. Again, we see that the contribution from contact interactions is substantial in order to get an equation of state compatible with microscopic calculations. The fit parameters in the present case are  $t_0 = -346.64$  and  $t_3 = 5255.08$  and they differ from those in isospin-symmetric nuclear matter due to the isospin dependence of the nuclear force.

Finally, we report our result on the dependence of the symmetry energy  $S$  on density in nuclear matter in Fig. 7. The empirical value of  $S$  at the saturation point is  $S(n_0) = 32.5 \text{ MeV}$  and we find the value  $S(n_0) = 35.1$ , which is a consequence of the fit to the neutron matter equation of state.

### V. CONCLUSIONS

In this work we have combined the methods of TFT and chiral Lagrangians to compute the self-energy of nucleons to leading order in the chiral expansion. In doing so, we have maintained the covariance of the pion and nucleon propagators and we have imposed self-consistency by solving a Schwinger-Dyson equation for the nucleon

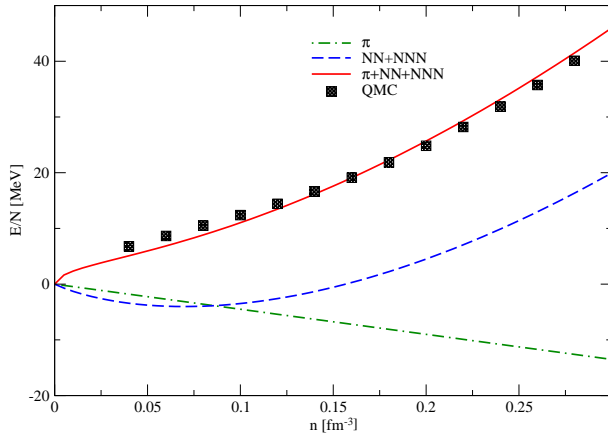


FIG. 6. (Color online) Dependence of the energy per particle in pure neutron matter on density at  $T = 0$  (solid red line). The contribution from chiral one-pion exchange is shown by the dash-dotted (green) line and that from the contact interactions by the dashed (blue) line.

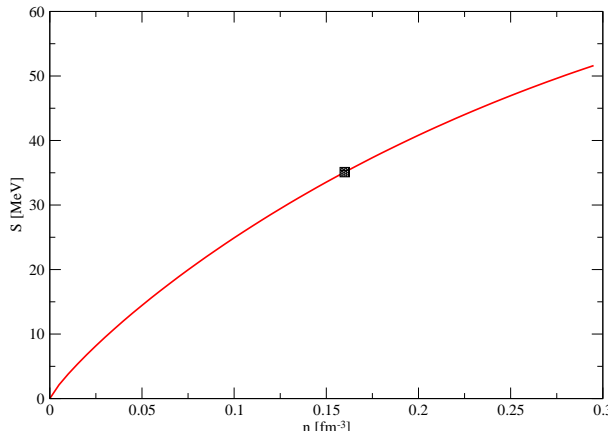


FIG. 7. Dependence of the symmetry energy of nuclear matter on density at  $T = 0$ .

self-energy. Medium- and short-range interactions between nucleons are represented by two- and three-body contact interactions which are chosen to have the structure of the corresponding terms in Skyrme density func-

tionals. These were then fitted to reproduce the nuclear saturation in the case of isospin-symmetric nuclear matter.

We find that the relativistic one-pion exchange contributes about half of the saturation energy for isospin-symmetric nuclear matter, the remainder being provided by two- and three-body contact interactions. By fitting the contact interactions to the saturation point for isospin-symmetric nuclear matter, our model produces reasonable values of the compressibility modulus. A comparison between our results and those obtained from a  $V_{\text{low-}k}$  interaction shows a good agreement for the attractive contribution to the energy per nucleon for isospin-symmetric nuclear matter.

Our approach has also been applied to pure neutron matter with similar results: the relativistic one-pion contribution needs to be supplemented with two and three-body contact interactions in order to match an equation of state derived from microscopic calculations.

Clearly, to obtain a consistent phenomenology of both isospin-symmetric nuclear and pure neutron matter, one needs to introduce contact interactions which account for the short-range attraction at the two-body level, as well as for three-body repulsion. In this respect further steps might be undertaken to resolve the relativistic dynamics of pions by including higher-order terms in the chiral expansion and incorporating  $\Delta$ -isobar excitations.

Methodologically, our approach differs from similar works since we address the nuclear equation of state with a chiral Lagrangian keeping a relativistic framework, and at the same time we impose self-consistency by solving a Schwinger-Dyson equation.

The in-medium electromagnetic and weak interactions of nucleons can be computed in a relativistically covariant manner starting from the self-consistent propagators derived above.

## ACKNOWLEDGMENTS

This work was partially supported by the HGS-HIRe graduate program at Frankfurt University (G. C.). We thank E. S. Fraga, R. D. Pisarski and J. Schaffner-Bielich for discussions.

---

[1] R. B. Wiringa, V. G. J. Stoks, and R. Schiavilla, Phys. Rev. C **51**, 38 (1995), arXiv:nucl-th/9408016; V. Stoks, R. Klomp, C. Terheggen, and J. de Swart, Phys. Rev. C **49**, 2950 (1994), arXiv:nucl-th/9406039 [nucl-th]; R. Machleidt, Phys. Rev. C **63**, 024001 (2001), arXiv:nucl-th/0006014 [nucl-th]; M. Lacombe, B. Loiseau, J. Richard, R. Vinh Mau, J. Cote, *et al.*, Phys. Rev. C **21**, 861 (1980).

[2] S. Weinberg, Phys. Lett. **B251**, 288 (1990); Nucl. Phys. **B363**, 3 (1991); C. Ordóñez, L. Ray, and U. van Kolck, Phys. Rev. C **53**, 2086 (1996); R. Machleidt and D. R. Entem, Physics Report **503**, 1 (2011), arXiv:1105.2919 [nucl-th]; E. Epelbaum, H.-W. Hammer, and U.-G. Meißner, Reviews of Modern Physics **81**, 1773 (2009), arXiv:0811.1338 [nucl-th].

[3] A. Akmal, V. R. Pandharipande, and D. G. Ravenhall, Phys. Rev. C **58**, 1804 (1998), arXiv:hep-ph/9804388;

O. Benhar, V. R. Pandharipande, and S. C. Pieper, *Reviews of Modern Physics* **65**, 817 (1993); S. Gandolfi, F. Pederiva, S. Fantoni, and K. E. Schmidt, *Physical Review Letters* **98**, 102503 (2007), arXiv:nucl-th/0607022; S. Gandolfi, A. Y. Illarionov, S. Fantoni, J. C. Miller, F. Pederiva, and K. E. Schmidt, *Monthly Notices of the Royal Astronomical Society: Letters* **404**, L35 (2010).

[4] B. D. Day and R. B. Wiringa, *Phys. Rev. C* **32**, 1057 (1985); D. Gambacurta, L. Li, G. Colò, U. Lombardo, N. Van Giai, and W. Zuo, *Phys. Rev. C* **84**, 024301 (2011); H.-J. Schulze and T. Rijken, *Phys. Rev. C* **84**, 035801 (2011); A. Sedrakian, *Prog. Part. Nucl. Phys.* **58**, 168 (2007), arXiv:nucl-th/0601086 [nucl-th]; F. Sammarruca, ArXiv e-prints (2011), arXiv:1111.0695 [nucl-th].

[5] K. Hebeler, S. K. Bogner, R. J. Furnstahl, A. Nogga, and A. Schwenk, *Phys. Rev. C* **83**, 031301 (2011); K. Hebeler and A. Schwenk, *Phys. Rev. C* **82**, 014314 (2010); A. Lacour, J. Oller, and U.-G. Meißner, *Annals of Physics* **326**, 241 (2011).

[6] J.-P. Blaizot and J.-Y. Ollitrault, *Phys. Rev. D* **48**, 1390 (1993), arXiv:hep-th/9303070; J.-P. Blaizot, E. Iancu, and A. Rebhan, *Phys. Rev. D* **63**, 065003 (2001), arXiv:hep-ph/0005003.

[7] S. Weinberg, *Physica A Statistical Mechanics and its Applications* **96**, 327 (1979).

[8] D. B. Kaplan, M. J. Savage, and M. B. Wise, *Nuclear Physics B* **478**, 629 (1996), arXiv:nucl-th/9605002.

[9] E. S. Fraga, Y. Hatta, R. D. Pisarski, and J. Schaffner-Bielich, *Phys. Rev. C* **69**, 035211 (2004), arXiv:nucl-th/0303019.

[10] B. Friman and C. Appel, *Physics Letters B* **474**, 7 (2000), arXiv:nucl-th/9907078.

[11] N. Kaiser, S. Fritsch, and W. Weise, *Nuclear Physics A* **697**, 255 (2002), arXiv:nucl-th/0105057; *Nuclear Physics A* **700**, 343 (2002), arXiv:nucl-th/0108010; W. Weise, *Progress in Particle and Nuclear Physics* **67**, 299 (2012), arXiv:1201.0950 [nucl-th].

[12] J. Gasser and H. Leutwyler, *Nuclear Physics B* **307**, 763 (1988).

[13] J. I. Kapusta, *Finite-temperature field theory., by Kapusta, J. I.. Cambridge University Press, Cambridge (UK), 1989, 229 p., ISBN 0-521-35155-3* (1989).

[14] P. Gögelein, E. N. E. van Dalen, C. Fuchs, and H. Müther, *Phys. Rev. C* **77**, 025802 (2008), arXiv:0708.2867 [nucl-th].

[15] S. Gandolfi, A. Y. Illarionov, K. E. Schmidt, F. Pederiva, and S. Fantoni, *Phys. Rev. C* **79**, 054005 (2009).